ORGANOMETALLICS

pubs.acs.org/Organometallics Article

Mechanism of 8-Aminoquinoline-Directed Ni-Catalyzed C(sp^3)−H Functionalization: Paramagnetic Ni(II) Species and the Deleterious Effect of Carbonate as a Base

Junyang Liu and Samuel A. Johnson*

Cite This: https://doi.org/10.1021/acs.organomet.1c00265 Read Online

ACCESS | Metrics & More | Article Recommendations | Supporting Information

ABSTRACT: Studies into the mechanism of 8-aminoquinoline-directed nickel-catalyzed C(sp^3)−H arylation with iodoarenes were carried out, to determine the catalyst resting state and optimize catalytic performance. Paramagnetic complexes undergo the key C−H activation step. The ubiquitous base Na_2CO_3 is found to hinder catalysis; replacement of Na_2CO_3 with NaO^{t}Bu gave improved catalytic turnovers under milder conditions. Deprotonation of the 8-aminoquinoline derivative *N*-(quinolin-8-yl)-pivalamide (**1a**) at the amide nitrogen using NaH, followed by reaction with $NiCl_2(PPh_3)_2$ allowed for the isolation of complex Ni([AQ^{piv}]-$\kappa N,N$)$_2$ (**3**) with chelating N-donors (where [AQ^{piv}] = $C_9NH_6NCO^tBu$). Complex **3** is a four-coordinate disphenoidal high-spin Ni(II) complex, excluding short anagostic Ni--^{t}Bu hydrogen interactions. Complex **3** reacts with the paddle-wheel [$Ph_3PNi(\mu$-$CO_2{}^tBu)_2]_2$ (**6·PPh$_3$**) or ^{t}BuCO$_2$H to give insoluble {[AQ^{piv}]Ni(O_2C^tBu)}$_2$ (**5**). Dissolution of **5** in donor solvents L (L= DMSO and DMF) gave a paramagnetic intermediate assigned by NMR as [AQ^{piv}]Ni(O_2C^tBu)L (**5·L**) and equilibrium reformation of **3** and **6·L**. DFT calculations support this equilibrium in solution. Both **3** and **5** undergo C−H activation at temperatures as low as 80 °C and in the presence of PR_3 (PR_3 = PPh_3, P^{i}Bu$_3$) to give Ni($C_9NH_6NCOCMe_2CH_2$-$\kappa N,N,C$)PR_3 (**7·PR$_3$**). The C−H functionalization reaction orders with respect to **7·P^{i}Bu$_3$**, iodoarenes, and phosphines were determined. Hammett analysis using electronically different aryl iodides suggests a concerted oxidative addition mechanism for the C−H functionalization step; DFT calculations were also carried out to support this finding. When Na_2CO_3 is used as the base, the rate determination step for C−H functionalization appears to be 8-aminoquinoline deprotonation and binding to Ni. The carbonate anion was also observed to provide a deleterious NMR-inactive low-energy off-cycle resting state in catalysis. Replacement of Na_2CO_3 with NaO^{t}Bu improved catalysis at milder conditions and made carboxylic acid and phosphine additives unnecessary. Complex **3** and its functionalized analogues were observed as the catalyst resting state under these conditions.

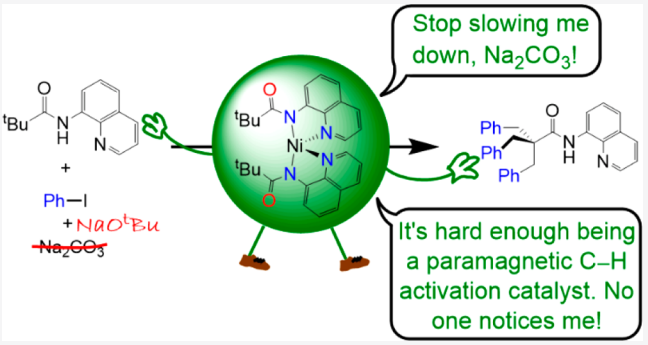

INTRODUCTION

The functionalization of C−H bonds provides an atom efficient way to construct new bonds to carbon. Transition metal complexes are often employed as catalysts to effect C−H bond transformations, with the precious metals often yielding the most active catalysts.[1−13] The use of abundant first-row transition metal catalysts in lieu of precious metals has received widespread attention, due to reduced cost and environmental benefits.[14] However, the first-row transition metals often feature decreased reactivity and selectivity in the functionalization of unactivated C(sp^3)−H bonds.[15]

Among the strategies developed to overcome these challenges,[16] one of the most successful methods is the installation of a directing group on the target molecule to aid selective C−H activation.[17] An early example is the nickelocene-mediated C−H activation of one of *ortho*-C−H bond of azobenzene.[18] In the 1990s, Chatani reported the Ru-catalyzed addition of alkenes to the *ortho*-C−H of aromatic ketones.[19] Seminal work done by Daugulis et al. in 2005 showed that *N,N*-bidentate directing groups such as 8-aminoquinoline (8-AQ) could be used to enhance the selectivity of Pd-catalyzed functionalization of C−H bonds.[20] In 2011, Chatani et al. demonstrated the first example of a Ni-catalyzed 8-AQ-directed C(sp^2)−H alkynylation reaction.[21] Related works soon followed, including C−C(sp)/C(sp^2)/C(sp^3)[22−43] and C−heteroatom bond formation.[22,44−56]

Received: April 30, 2021

https://doi.org/10.1021/acs.organomet.1c00265
Organometallics XXXX, XXX, XXX−XXX

Scheme 1. General Reaction Scheme, Proposed Mechanisms, and Isolated Analogue of Intermediate and Proposed Resting State[a]

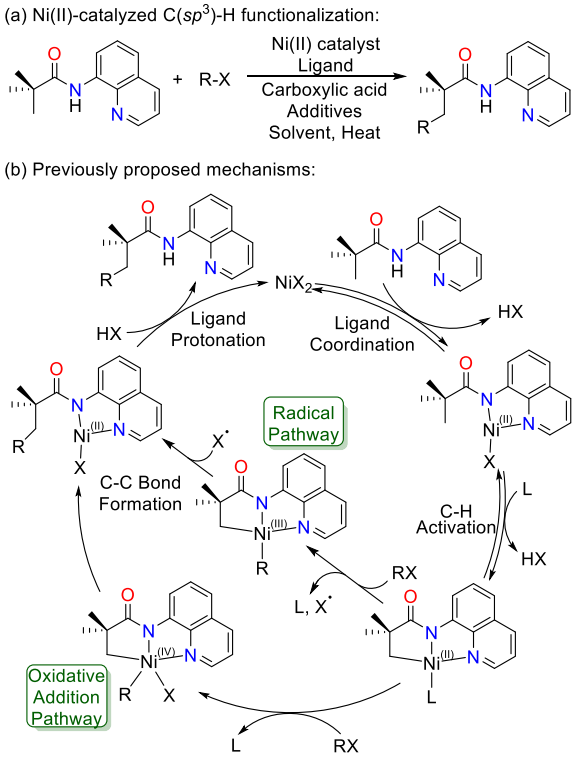

[a](a) General reaction scheme of 8-AQ-assisted Ni(II)-catalyzed C(sp^3)—H functionalization. (b) Proposed mechanisms based on previous computational studies. (c) Isolated analogue of catalytically-relevant intermediate and DFT-proposed diamagnetic catalyst resting state.

The activation of the weaker C—H bonds of alkyl groups is typically more difficult for Ni than the stronger aromatic C—H bonds. The first example employing 8-AQ as a directing group in the more difficult Ni-catalyzed C(sp^3)—H functionalization was not reported in literature until 2014[23] and used aryl iodides as coupling partners. Although the mechanism of Pd-catalyzed C(sp^3)—H functionalization reactions are well-studied,[57−59] less is known about the possible differences in Ni-catalyzed systems. An understanding of the catalytic cycle and its elementary steps are crucial for the designing of new catalyst systems with improved selectivity and efficiency. Multiple mechanisms have been suggested for Ni-catalyzed C(sp^3)—C bond formation, including oxidative addition and radical pathways shown in Scheme 1a,b. DFT calculations have suggested that both mechanisms are operational depending on the nature of the substrates.[60,61] Love and co-workers published a study on the C—H activation step using an 8-AQ functionalized tertiary urea as the model substrate and isolated a Ni(II) ureate complex with a C—Ni bond, as shown in Scheme 1c.[62] The intramolecular C—H activation is suggested to proceed via a concerted metalation deprotonation mechanism with an electrophilic C—H activation transition state, as supported by Hammett plot and KIE studies;[62] however, no intermediates prior to C—H activation or functionalization steps have been isolated. DFT studies suggest a diamagnetic Ni(II) complex prior to C—H activation as the catalytic resting state shown in Scheme 1c,[61] but no experimental attempt to verify this theoretical prediction has been reported to date.

Herein, we report a mechanistic study of 8-AQ-directed, Ni-catalyzed C(sp^3)—H arylation with aryl halides with the identification and isolation of unexpected mono- and dinuclear paramagnetic nickel intermediates. The results suggest a more complex mechanistic manifold involving paramagnetic intermediates, and a reconsideration of the rate-determining step in this catalytic functionalization, which counter to DFT predictions involves neither the expected C—H activation nor Ni(II)—Ni(IV) oxidative addition, but rather the deprotonation step, when Na_2CO_3 is used as the base. Furthermore, evidence not only proves that Na_2CO_3 is an insufficient base but also suggests the carbonate anion forms an off-cycle resting state that is detrimental to catalyst performance, and replacement with NaO^{t}Bu leads to more efficient catalysis.

RESULTS AND DISCUSSION

Ligand Coordination. Attempts were made to coordinate *N*-(quinolin-8-yl)pivalamide, abbreviated [AQ^{piv}]H (**1a**), to a variety of Ni(II) sources, to generate a Ni(II) complex prior to C—H bond activation. Under catalytic conditions, the ligand coordination step has been proposed to proceed through base-mediated deprotonation of the amido nitrogen to generate the anionic ligand precursor [AQ^{piv}]Na (**2a**), followed by a transmetalation with Ni(II) salts. However, the reaction between **1a** and NiX_2 sources in refluxing THF or toluene (X = OTf, Cl, Br, I, and acetylacetonate) in the presence of excess Na_2CO_3 provided no observable reaction. Similarly, the

Scheme 2. Synthesis of Sodium Salt [AQ^{piv}]Na (2a) and Reaction to Give Ni[AQ^{piv}]$_2$ (3)[a]

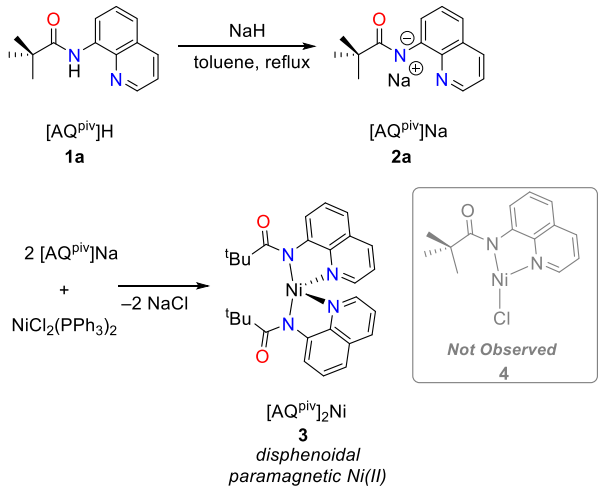

[a]Complex **4** was not observed by ^{1}H NMR, irrespective of reaction stoichiometry.

https://doi.org/10.1021/acs.organomet.1c00265
Organometallics XXXX, XXX, XXX−XXX

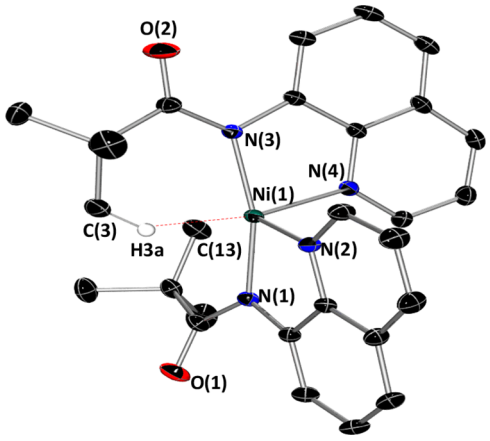

Figure 1. ORTEP depiction of **3** (CCDC 2055354) with 30% thermal ellipsoids. Hydrogens except the one closest to Ni were omitted for clarity. Selected bond lengths (Å): Ni(1)−N(1) 1.981(1), Ni(1)−N(2) 1.982(1), Ni(1)−N(3) 1.983(1), Ni(1)−N(4) 1.974(1), Ni(1)−H(3a) 2.17. Selected bond angles (deg): N(1)−Ni(1)−N(3) 165.88(6), N(3)−Ni(1)−N(4) 84.13(5), N(1)−Ni(1)−N(2) 84.28(6), N(2)−Ni(1)−N(4) 95.29(6).

Scheme 3. Synthesis of 3-d_6 Used in Probing Potential Agostic Interactions in 3 by Comparison of Me Group ^{1}H NMR Chemical Shifts[a]

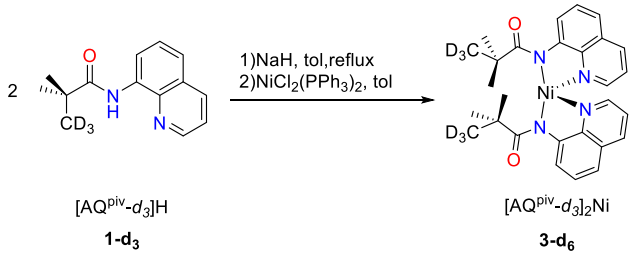

[a]No shift associated with an isotopic perturbation of equilibrium was observed.

reaction with Na_2CO_3 showed no evidence for the deprotonation of **1a** under these conditions; however, the stronger base NaH gave quantitative conversion to isolable sodium salt **2a**, as shown in the top of Scheme 2. Sodium salt **2a** is insoluble in THF and was characterized by NMR spectroscopy in DMSO.

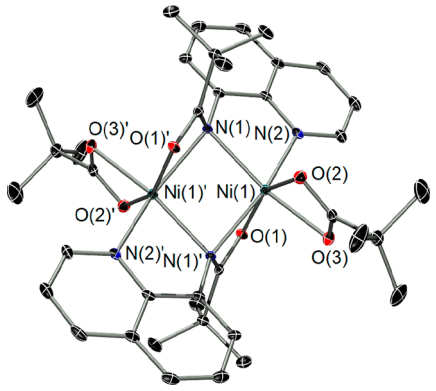

Figure 2. ORTEP depiction of the solid-state molecular structure of **5** (CCDC 2055455) with 30% thermal ellipsoids. Hydrogens are omitted for clarity. Selected bond lengths (Å): Ni(1)−N(1) 2.134(4), Ni(1)−N(1)′ 2.174(6), Ni(1)−N(2) 2.030(7), Ni(1)−Ni(1)′ 3.014(2), Ni(1)−O(1) 2.069(4), Ni(1)−O(2) 2.083(4), Ni(1)−O(3) 2.080(4). Selected bond angles (deg): Ni(1)−N(1)−Ni(1)′ 88.8(2), O(1)−Ni(1)−O(2) 155.8(2), N(1)−Ni(1)−N(1)′ 91.2(2), O(2)−Ni(1)−O(3) 63.3(2), N(1)−Ni(1)−N(2) 81.2(2).

Salt metathesis between **2a** and $NiCl_2(PPh_3)_2$ in toluene led exclusively to the formation of the dark brown paramagnetic complex $[AQ^{piv}]_2Ni$ (**3**), as shown in the bottom of Scheme 2. The reaction was monitored by ^{1}H NMR, and the conversion was practically quantitative within 30 min at room temperature. Analogous reactions with other Ni(II) precursors such as $NiCl_2(P^iBu_3)_2$ or $NiCl_2$ also provided **3**, but these reactions required 12 h to go to completion. Complex **3** is pentane-insoluble and was crystallized from toluene at −40 °C Although the monoligated complex $[AQ^{piv}]NiCl$ (**4**) is related to key intermediates in proposed catalytic cycles, it was not observed in these reactions. Even using substoichiometric **2a** (e.g., 0.5 equiv), only complex **3** was observed. This is almost certainly due to the thermodynamic instability of **4** with respect to ligand redistribution to give **3**.

Scheme 4. Synthesis Routes to 5, the Paramagnetic and Dinuclear Forms of the Previously Proposed Mononuclear Species $[AQ^{piv}]Ni(O_2C^tBu)$

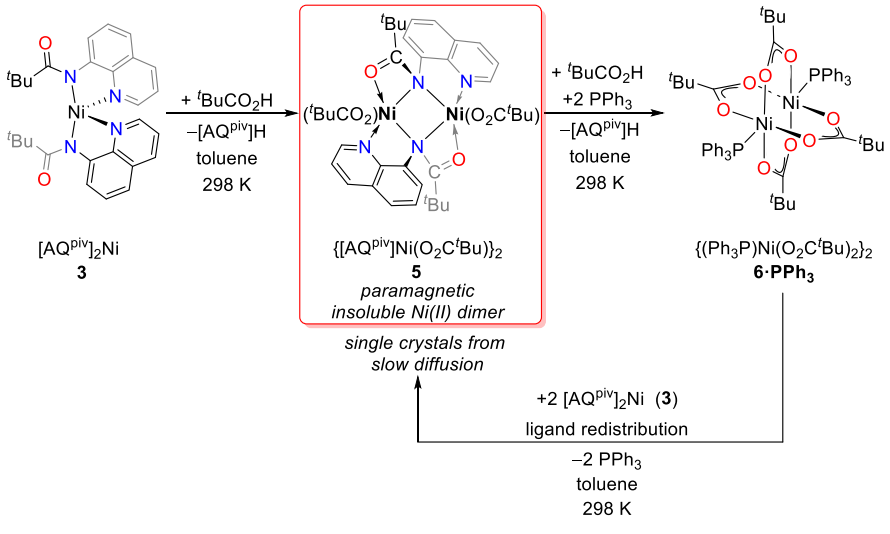

https://doi.org/10.1021/acs.organomet.1c00265
Organometallics XXXX, XXX, XXX−XXX

Scheme 5. Reaction of Dinuclear 5 with Donor Solvents to Give an Equilibrium Mixture of the Paramagnetic Species mono-5·L, 3, and 6 (L = DMSO and DMF)

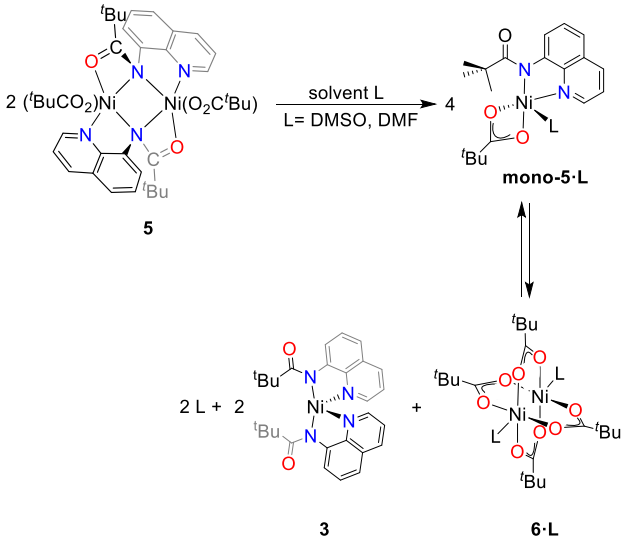

Scheme 7. Synthesis of C−H Activated Adducts 7·PR$_3$ and Alternate Salt Metathesis Route[a]

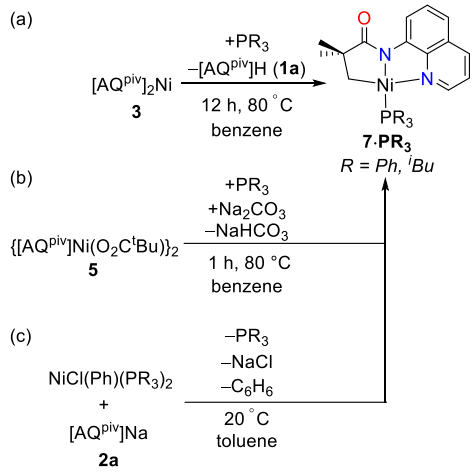

[a]Synthesis of C−H activated adducts **7·PR$_3$** from (a) complex **3** or (b) complex **5**. (c) Alternate salt metathesis route to **7·PR$_3$** with room-temperature loss of benzene in the C−H activation step.

Paramagnetic Ni(II) complexes are often observable by ^{1}H NMR, and the spectrum of **3** is typical for a paramagnetic species. The chemical shifts for **3** span from 5 to 220 ppm, and all the resonances are broad singlets. The ^{1}H NMR peak at δ 64 is readily assigned as the ^{t}Bu group due to its integration to 18 H. The ^{13}C NMR peak assigned to the ^{t}Bu methyl groups

Scheme 6. Calculated Gibbs Free Energies and Enthalpies for Solvation of 5 with DMSO[a]

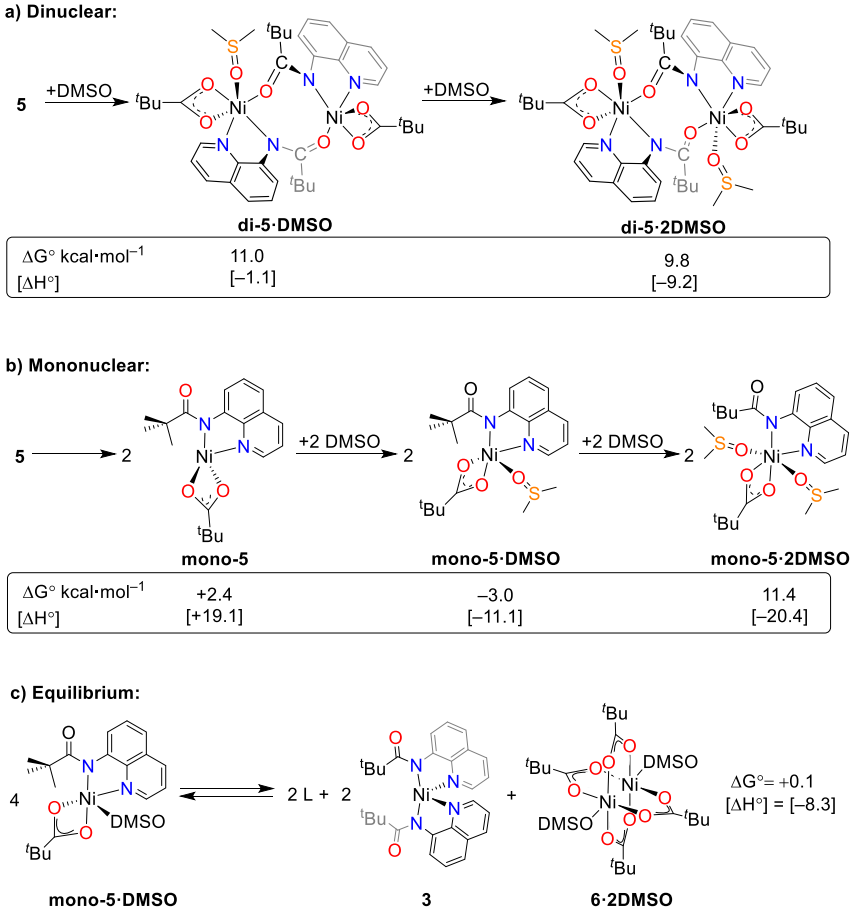

[a]Giving (a) dinuclear complexes and (b) mononuclear complexes. Only the formation of **mono-5·DMSO** is favorable. (c) The calculated energetics of the experimentally observed equilibrium between **mono-5·DMSO** and **3** and **6·2DMSO** in DMSO.

https://doi.org/10.1021/acs.organomet.1c00265
Organometallics XXXX, XXX, XXX−XXX

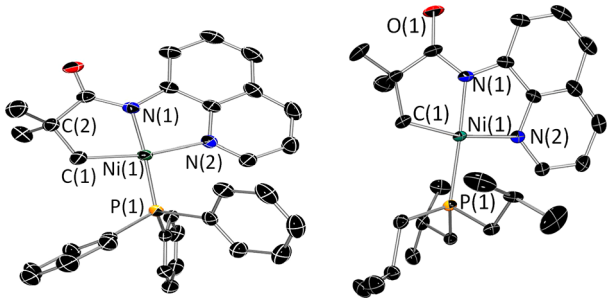

Figure 3. ORTEP depictions of **7·PPh$_3$** (CCDC 2055449) and **7·P^{i}Bu$_3$** (CCDC 2055446), with 30% thermal ellipsoids.

Scheme 8. Reaction of 7·P^{i}Bu$_3$ with PhI in the Presence of 1a to Give 3, 8 (CCDC 2055459), and 9

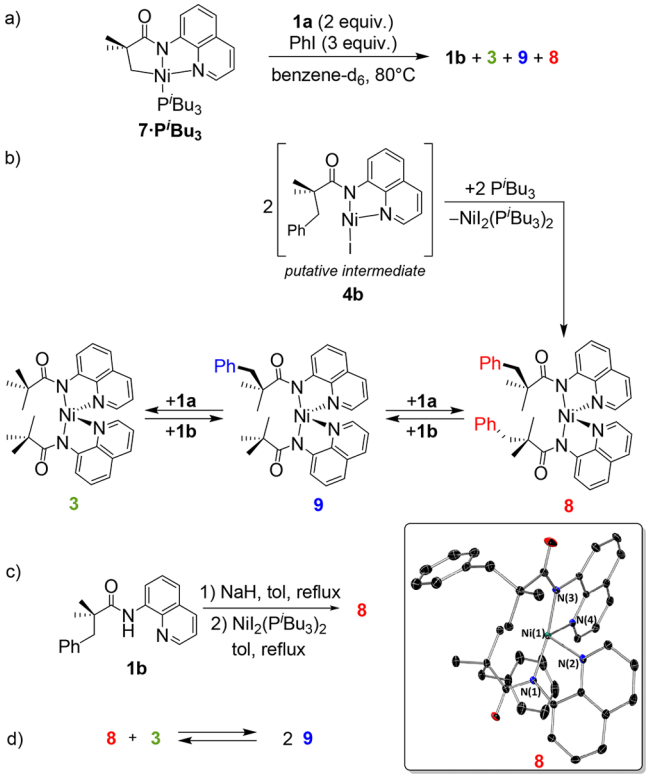

was observed at δ 622.6. The magnetic moment (μ_{eff}) of **3** was determined to be 3.31 μ_B by Evan's method at 298 K in benzene-d_6, which corresponds to a high spin Ni(II) bearing two unpaired electrons with spin−orbit coupling (S = 1, spin only μ_{eff} = 2.83 μ_B).

Single-crystal X-ray diffraction provided structural data for **3**, and an ORTEP depiction is shown in Figure 1. The nickel center adopts a rare seesaw geometry; only a few examples of disphenoidal Ni(II) complexes are known.[63−66] There are few relevant structurally characterized examples of complexed 8-AQ ligand moieties where the ligand has not already undergone C−H activation. Previously, phenyl C(sp^2)−H activated complexes have been isolated as penta-coordinated complexes with one C(sp^2)−H bond activated for Ni and Co-catalyzed systems.[67−69] A single Cu(II) complex in known without activation for bis[*N*-(quinolin-8-yl)benzamidato-κ^2N,N']copper(II).[70]

Notable in the structure is the close proximity between Ni(1) and H(3a) on the ^{t}Bu group, which is only 2.17 Å. This short contact is drawn as a red dashed line in Figure 1. The second ^{t}Bu group features a second contact with a slightly longer distance of 2.32 Å. If there were attractive agostic interactions with both ^{t}Bu groups, then complex **3** would be octahedral. However, all evidence suggests that these are anagostic interactions. The IR spectrum of **3** shows show no reduced C(sp^3)−H stretching mode. The ^{t}Bu resonance gave a single signal in the ^{1}H NMR at temperatures as low as 193 K, though this could arise from a rapid fluxional process where each methyl hydrogen in each methyl group on the ^{t}Bu substituents adopt the agostic position.[71] Equilibrium isotope effects should be very sensitive in this paramagnetic system. As shown in Scheme 3, complex [AQ^{piv}-d_3]$_2$Ni (**3-d_6**) was prepared from the deuterium-labeled ligand [AQ^{piv}-d_3]H (**1a-d_3**). For an attractive agostic complex, there should be a preference for the protons to occupy the agostic positions,[72] which should give a chemical shift change compared to **3**;[73,74] this isotopic perturbation of equilibrium is a powerful technique for the assignment of agostic interactions in rapidly fluxional complexes. Both agostic[75−78] and anagostic[79,80] complexes of Ni(II) have been reported. The ^{1}H NMR chemical shifts of **3** and **3-d_6** are indistinguishable, which supports that the short H−Ni distances in **3** are nonattractive anagostic interactions.

Carboxylate Complexes. Carboxylic acids are a commonly employed additive in 8-AQ-directed Ni-catalyzed C(sp^3)−H functionalization. The carboxylate has been proposed to play an important role in C−H activation and subsequent proton transfer. Paramagnetic complexes of the type [AQ^{piv}]Ni(O$_2$C^{t}Bu) have been proposed as an intermediate and resting state in the catalytic cycle, but never isolated.[62] The reaction of carboxylic acids with **3** was envisioned as a synthesis route to these speculative paramagnetic Ni(II) precursors to C−H activation.

The reaction between **3** and 1 equiv of ^{t}BuCO$_2$H in toluene or THF at room temperature caused an immediate loss of the dark brown color of **3** in solution and the formation of {[AQ^{piv}]Ni(O$_2$C^{t}Bu)}$_2$ (**5**) as a green microcrystalline precipitate, as shown in Scheme 4. Protonolysis of the second [AQ^{piv}] ligand by addition of a second equivalent of ^{t}BuCO$_2$H in the presence of PPh$_3$ generates the paddle-wheel complex (**6-PPh$_3$**), shown on the right side of Scheme 4.

Complex **5** proved insoluble in common polar organic solvents such as THF or CH$_2$Cl$_2$. Crystals of **5** suitable for X-ray diffraction were grown from slow diffusion of layered toluene solutions of **3** and **6** which undergo slow ligand exchange to generate **5**, as shown in the bottom right of Scheme 4. This reaction also proceeds with [(Et$_3$N)Ni(O$_2$C^{t}Bu)$_2$]$_2$ in lieu of **6**. An ORTEP depiction of the solid-state molecular structure of **5** is shown in Figure 2. Complex **5** could also be obtained via salt metathesis between **6** with [AQ^{piv}]Na, but the reaction of **6** with [AQ^{piv}]H without an added base yielded no observable reaction.

Previously structurally characterized examples containing derivatives of 8-AQ are monometallic species.[81] Contrary to previously published mechanistic DFT calculations that predicted **5** should be a mononuclear square planar complex, **5** exhibits a dimeric structure with each nickel center adopting a distorted octahedral geometry. The structure of **5** has crystallographically imposed inversion symmetry. The amido nitrogens N(1) and N(1)′ bridge the two Ni centers. The carbonyl groups bend perpendicular from the plane of the 8-AQ moieties, allowing the O(1)′ oxygen atom to chelate to a

https://doi.org/10.1021/acs.organomet.1c00265
Organometallics XXXX, XXX, XXX−XXX

Scheme 9. (a) Reaction Conditions for Pseudo-First-Order Kinetics Study of 7·P^{i}Bu$_3$ with *para*-Substituted Aryl Iodides to Give 1-R and (b) Hammett Plot Comparing Initial Rates of Arylation

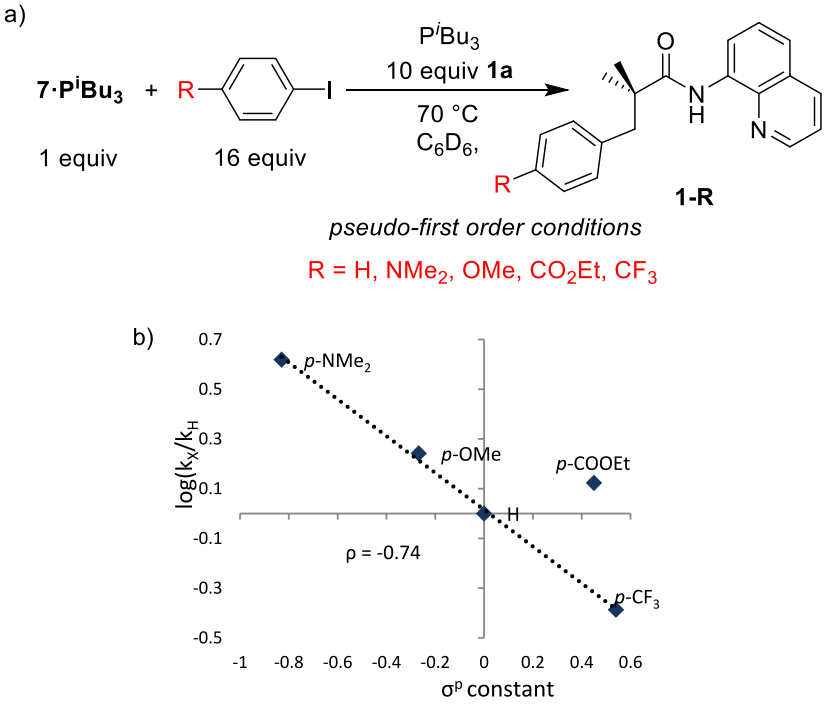

different nickel than does N(2). This represents the first isolated example of the proposed catalytically relevant nickel carboxylate intermediate prior to C−H activation. Dinuclear nickel species have been known to mediate the activation of a number of C−atom (O, H, and X) bonds,[82,83] and the possibility of **5** participating in the catalytic cycle cannot be ruled out, despite its poor solubility. It has been previously reported that the reaction of $[(Et_3P)Ni(OPiv)_2]_2$ with an 8-AQ urea derivative provided a paramagnetic intermediate that underwent C−H bond activation, though its identity was not ascertained.[62]

Insolubility rendered the determination of solution NMR data for **5** impossible. Green complex **5** reacts over an hour in the donor solvents DMSO and DMF to give brown solutions. In both solvents, this provides a complex tentatively assigned by NMR as $[AQ^{piv}]Ni(O_2C^tBu)L$ (**mono-5·L**), the mononuclear solvated form of **5**, which is in equilibrium with complex **3** and paddle-wheel complex **6·L** (L = DMSO and DMF), as shown in Scheme 5. Complex **3** was assigned by ^{1}H NMR by comparison to a sample of isolated **3** dissolved in DMSO, and complex **6·DMSO** was assigned by comparison to a DMSO solution of paddle-wheel complex $[Ni(O_2C^tBu)_2NEt_3]_2$, which appeared to generate $[Ni(O_2C^tBu)_2(DMSO)]_2$. The only remaining ^{1}H NMR resonances for the equilibrium solution that were not assignable to **3** or **6·PPh$_3$** were assignable to **mono-5·DMSO**. Complex **mono-5·DMSO** features broad paramagnetic shifted resonances, similar to **3**, but with an added ^{t}Bu resonance for the O_2C^tBu moiety at δ 8.2 that integrates to 9H and has the same integral as the ^{t}Bu resonance for AQ^{piv} in **mono-5·DMSO** at δ 72.7. It should be restated that in the absence of DMF or DMSO, the reaction of **6·PPh$_3$** and **3** can be used to generate dinuclear **5**, suggesting the presence of the donor solvents influences this equilibrium. Confirmation of this was achieved by the reaction of **6·PPh$_3$** and **3** in DMF or DMSO, which generates the same equilibrium mixture with **mono-5·L** as the dissolution of dinuclear **5** in these solvents.

The NMR assignment of **mono-5·L** is tentative because it proved impossible to assign resonances for the coordinated solvent. In principle, this species could be mononuclear with multiple coordinated solvent molecules rather than one or could be a dinuclear solvated species. In order to probe the likely identity of **mono-5·L** and the energetics of the equilibria exhibited by **5** in donor solvents, DFT calculations were carried out. Both mononuclear and dinuclear forms of **5** were optimized with one or two O-bonded DMSO or DMF coordinated to the nickel centers and are summarized in Scheme 6. The binding of a single DMSO molecule to dinuclear **5** gives **di-5·DMSO** and is calculated to be 11.0 kcal·mol^{-1} uphill, where the energy given is a ΔG° for the transformation in the gas phase. The binding of two solvent molecules to **5** gives **di-5·2DMSO**, which has a Gibbs free energy change of +9.8 kcal·mol^{-1}; neither dinuclear species appears viable as the species observed in solution due to these strongly disfavored reaction thermodynamics, shown in Scheme 6a.

Mononuclear forms proved more favorable, as shown in Scheme 6b. The dissociation of dinuclear **5** into its mononuclear form $[AQ^{piv}]Ni(O_2C^tBu)$ (**mono-5**) without coordination of a solvent had a favorable ΔG° of −0.3 kcal·mol^{-1}. Although this seems to suggest that **mono-5** should be observable, it should be noted that DFT calculations overestimate the entropic component for solution phase reactions, and dinuclear **5** is insoluble in most solvents. The reaction of 5 with DMSO to generate the monosolvated species **mono-5·DMSO** has a more favorable ΔG° of −3.0 kcal·mol^{-1} for its most stable isomer. Coordination of a second DMSO to give **mono-5·2DMSO** was strongly disfavored, with the most stable isomer having a ΔG° of +11.4 kcal·mol^{-1}. These calculations support the assignment of the solution

https://doi.org/10.1021/acs.organomet.1c00265
Organometallics XXXX, XXX, XXX−XXX

Scheme 10. DFT-Computed Pathway and Graph Showing Correlation between the Observed Rate and Calculated $\Delta G^{\ddagger}_{OA}$[a]

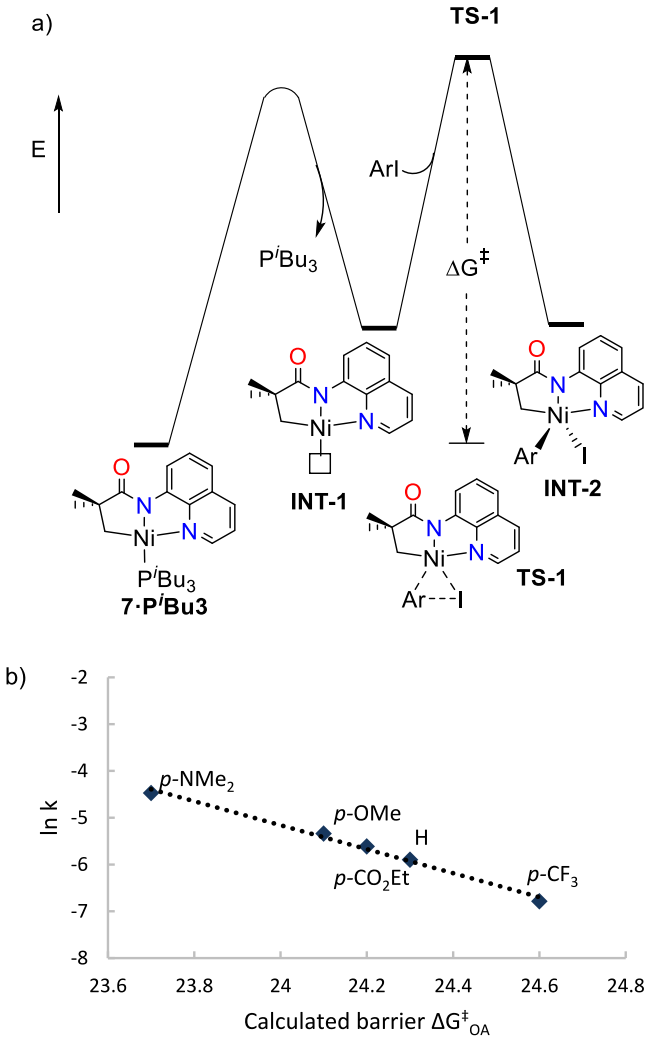

[a](a) DFT computed pathway of the oxidative addition reaction between iodoarenes and 7·P^{i}Bu$_3$ (details are in Supporting Information). (b) Graph showing correlation between the observed rate and calculated $\Delta G^{\ddagger}_{OA}$.

Scheme 11. Catalytic Arylation of Terminal C(sp^3)−H Bonds Using NaO^{t}Bu as the Base[a]

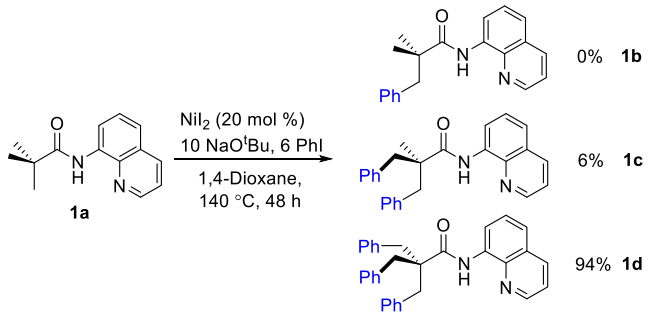

[a]Yields are determined by relative integration in the ^{1}H NMR.

species observed by ^{1}H NMR as AQ^{piv}]Ni(O$_2$C^{t}Bu)DMSO, **mono-5·DMSO**.

Calculations also showed that the equilibrium between **mono-5·DMSO** with **3** and **6·2DMSO** observed in solution was viable. The calculated ΔG° for this reaction was only 0.1 kcal·mol^{-1}, as shown in Scheme 6c.

The dissolution of complex **5** in DMF was also investigated computationally. The conclusion of the study with DMF proved identical to that with DMSO. The paramagnetic mononuclear monosolvated complex **mono-5·DMF** is predicted to be the favored form in solution, and exist in equilibrium with **3** and **6·2DMF.** The energies for these related complexes are provided in the Supporting Information.

C−H Activation. Both [AQ^{piv}]$_2$Ni (**3**) and {[AQ^{piv}]Ni(O$_2$C^{t}Bu)}$_2$ (**5**) undergo C−H activation when heated at 80 °C in benzene-d_6, even though **5** is insoluble. The C−H activated products **7·PR$_3$** (where PR$_3$ = PPh$_3$ and P^{i}Bu$_3$) could be isolated through the addition of an auxiliary ligand such as phosphines, as shown in Scheme 7. Multinuclear NMR spectroscopy showed that other coordinating solvents such as MeCN or DMSO also gave adducts tentatively assigned as **7·NCMe** and **7·DMSO**, but these could not be isolated as crystalline solids. Diamagnetic Pd analogues are known.[84−89] As shown in Scheme 7a), the C−H activation of **3** liberates 1 equiv of [AQ^{piv}]H (**1a**), which was observed by ^{1}H NMR spectroscopy. The C−H activation **5** in the absence of added base also produced **1a**, presumably because the ^{t}BuCO$_2$H produced by deprotonation of the C−H bond protonates unreacted **5**, generating [AQ^{piv}]H (**1a**), which lowers the yield. The addition of Na$_2$CO$_3$ in the C−H activation of **5** was an effective way to suppress this side reaction, as shown in Scheme 7b).

The formation of **7·PR$_3$** using **5** as precursor is an order of magnitude faster than **3** at 80 °C. Initial rates of reaction for the conversion of **3** to **7·PPh$_3$** in benzene-d_6 were examined over a range of 30 °C and an Eyring plot provided a $\Delta G^{\ddagger}$ of 23.1 kcal·mol^{-1}. A computational study by Lan utilizing bicarbonate anion as proton acceptor determined a barrier of 23.7 kcal·mol^{-1},[90] whereas in Liu's study, an anionic, DMF-coordinated sodium carbonate ligand drops the calculated barrier to 21.4 kcal·mol^{-1}.[61] The more rapid activation by **5** versus **3** supports that carboxylate lowers the C−H activation barrier; a similar effect of carboxylates on the rate of C−H activation are also reported in other transition-metal-catalyzed systems.[57,91−93] Multiple computational studies have pointed out that the C−H bond is further polarized by the carboxylate through noncovalent interactions in Pd-catalyzed systems.[94] However, as the solid structure has shown, the distance between the CH$_3$ groups and the carboxylate oxygen in **5** is much longer than a typical hydrogen bond length, suggesting rearrangement of the ^{t}Bu group or carboxylate ligand may occur prior to C−H activation; it is unclear at which Ni site the ^{t}Bu is activated relative to the coordinated carboxylate ligands, given that breaking the [AQ^{piv}] oxyen−nickel interaction in **5** could allow activation at either metal site in this dinuclear complex. Unfortunately, the instability and insolubility of **5** prevented us to study the detailed mechanism of C−H activation in solution.

Adducts **7·PR$_3$** were also conveniently synthesized at room temperature from reaction between [AQ^{piv}]Na (**2a**) and *trans*-NiCl(Ph)(PR$_3$)$_2$ (R = Ph and ^{i}Bu), as shown in Scheme 7c). This reaction combines transmetalation and C−H activation, which in this case with the Ni−Ph group acting as the base promotes very rapid C−H activation at room temperature. Single crystals of **7·PPh$_3$** and **7·P^{i}Bu$_3$** were grown from a

https://doi.org/10.1021/acs.organomet.1c00265
Organometallics XXXX, XXX, XXX−XXX

saturated THF and toluene solutions, respectively. The solid-state structures, depicted in Figure 3, indicate they are square planar and exhibit characteristic Ni−C bonds (1.929(3) Å for **7·PPh$_3$** and 1.935(3) Å for **7·P^{i}Bu$_3$**), similar to known complexes.[62,63,95−97] The different steric profiles of phosphine ligands does not have a significant influence on the bond angles, with a N(2)−Ni(1)−C(1) angle of 168.5(1)° for **7·PPh$_3$** and 166.9(1)° for **7·P^{i}Bu$_3$**].

Complexes **7·PR$_3$** are all diamagnetic and feature characteristic coupling of NiCH$_2$ to phosphorus in the ^{1}H NMR spectra of complexes **7·PPh$_3$** ($^3J_{HP}$ = 10.5 Hz) and **7·P^{i}Bu$_3$** ($^3J_{HP}$ = 6.5 Hz), consistent with coordination of the PR$_3$ in solution. The ^{31}P{^{1}H} NMR also features sharp singlets for **7·PPh$_3$** at δ 42.2 and **7·P^{i}Bu$_3$** at δ 5.2; these are observed downfield from the free PR$_3$ by approximately 50 ppm. The addition of free PPh$_3$ to **7·PPh$_3$** converts the ^{1}H NMR CH$_2$ doublet to a singlet, and the phosphorus peak broadens in the ^{31}P{^{1}H} NMR, consistent with rapid phosphine ligand exchange. In contrast, the addition of excess P^{i}Bu$_3$ to **7·P^{i}Bu$_3$** did not cause any evidence of fluxional exchange, even upon heating to 373 K in toluene-d_8.

C−H Functionalization. After C−H activation, the next step in the catalytic cycle is reaction of **7· PR$_3$** with aryl halides. In an attempt to observe intermediates, the pseudocatalytic condition reaction between **7·P^{i}Bu$_3$** and iodobenzene in the presence of **1a** in benzene-d_6 at 80 °C was monitored by NMR spectroscopy, as shown in Scheme 8a. No Ni(IV) complex from oxidative addition was observed; if involved, the Ni(IV) complex is likely a high energy intermediate. In addition to the formation of the organic arylated product **1b**, the distinctive paramagnetic peaks of complex **3** were observable early in the reaction. As increased conversion of **1a** to **1b** occurred, new peaks were observed for the complexes **8** and **9**, as shown in Scheme 8. Complexes **8** and **9** are analogues of **3** with arylated ligands, and feature many ^{1}H NMR chemical environments proximal to those for **3**. Complexes **3**, **8**, and **9** likely arise from ligand redistribution from putative intermediate **4b** shown central in Scheme 8b, similar to the chemistry of the unobserved complex **4** shown in Scheme 2. In the ^{31}P{^{1}H} NMR, the broad singlet at δ 5.0 for NiI$_2$(P^{i}Bu$_3$)$_2$ was also observed. Complexes **3**, **8**, and **9** are in equilibrium under the reaction conditions, with the relative proportion of each determined by the ratio of **1a** and **1b** in solution.

To confirm the identity of species **8** and **9**, initially assigned by ^{1}H NMR and analysis of equilibria, complex **8** was synthesized from NiCl$_2$(P^{i}Bu$_3$)$_2$ and ligand **1b**, as shown in Scheme 8c. The solid-state X-ray structure of **8** shows it is structurally similar to **3**, with a disphenoidal geometry at Ni. The ^{1}H NMR of **8** exhibits characteristic broad singlets for a paramagnetic Ni(II) species. Although the asymmetric complex **9** could not be isolated in a pure form, it could be prepared in equilibrium by the addition of **1a** to **8**, which demonstrates the validity of the equilibrium shown in Scheme 8b. Alternatively, a solution of **9** could be prepared by the equilibrium reaction of equimolar amounts of **3** and **8** via ligand redistribution. At 298 K this reaction proceeds over the course of hours.

To support the proposed Ni(II) to Ni(IV) oxidative addition mechanism for the functionalization step, the influence of aryl iodide on reaction rate was studied, as shown in Scheme 9a. Initial rate studies were carried out for these reactions of **7·P^{i}Bu$_3$** with aryl iodides to generate **1-R**. The reaction was done in the presence of excess **1a** to avoid the formation of diarylated products. In the initial stage (<30 min) of the reaction the rate can be conveniently determined from the formation of **1-R**. The reaction was found to be first-order with respect to both **7·P^{i}Bu$_3$** and iodobenzene but inverse first-order for P^{i}Bu$_3$. The inhibition by P^{i}Bu$_3$ suggests a mechanism where a pre-equilibrium phosphine dissociation occurs prior to reaction with aryl iodide. Iodobenzene was used in excess to give pseudo-first-order kinetics, and P^{i}Bu$_3$ was added to ensure a constant concentration for all reactions studied.

The electronic effect of *para*-substituents on the reaction rate was examined using iodoarenes bearing functional groups at the *para*-position. A Hammett plot was constructed, and a linear correlation with a ρ of −0.74 was observed for iodoarenes bearing *p*-NMe$_2$, *p*-OMe, *p*-H, and *p*-CF$_3$ substituents, as shown in Scheme 9b. In contrast to the positive ρ values often observed for oxidative addition to Ni(0) or Pd(0),[98,99] the negative ρ could be appropriate for oxidative addition to a Ni(II) center. Studies of the oxidative addition of aryl iodides to Pd(II) show ρ values of −0.77[100] and −0.85,[101] respectively, as electron-donating substituents are expected to stabilize Pd(IV) centers. Thus it is reasonable to think the more electrophilic Ni(II) will react faster with electron-rich arenes; however, Hammett studies of reactions involving concerted oxidative addition to Ni(II) are currently lacking for comparison. The small negative value of ρ rules out a rate-determining electron transfer, because ρ values for this mechanism would be expected to be near 2.0.[98] Addition of a radical scavenger such as TEMPO gave no decrease in the rate of formation of **1b**, which also suggests a radical pathway is unlikely. These experimental results support the results of computational studies by Liu[61] and Sunoj.[60]

The *p*-CO$_2$Et substituted arene is an obvious outlier in Scheme 9b, with a much faster rate of reaction than anticipated from the Hammett ρ value. To further understand this exception and whether a concerted mechanism is still operational with this substituent, DFT studies were carried out using Gaussian 16 to analyze both phosphine dissociation and oxidative addition steps with respect to **7·P^{i}Bu$_3$** that generates Ni(IV) intermediate **INT-2** through transition state **TS-1** (Scheme 10a). The reaction with 4-iodo-*N*,*N*-dimethylaniline (*p*-NMe$_2$) is calculated to have the lowest activation energy barrier with a $\Delta G^{\ddagger}_{OA}$ that is 0.6 kcal/mol lower than iodobenzene at 298 K. Calculation also revealed the reaction with ethyl 4-iodobenzoate also has a lower $\Delta G^{\ddagger}_{OA}$ than iodobenzene ($\Delta\Delta G^{\ddagger}_{OA}$ = −0.1 kcal mol^{-1}) and is slightly higher than 4-iodoanisole ($\Delta\Delta G^{\ddagger}_{OA}$ = 0.1 kcal mol^{-1}), which is in agreement with our experimental result and a higher rate of reaction is expected. A plot of calculated $\Delta G^{\ddagger}_{OA}$ against the natural log of the observed rate of each reaction was also constructed and a linear correlation was observed, suggesting the same mechanism was operative throughout the reactions with a series of substituted iodoarenes (Scheme 10b).

Catalyst Resting State and the Deleterious Effect of Na$_2$CO$_3$. Intuitively, one might anticipate either the C−H activation step or the oxidative addition to give Ni(IV) would be rate-limiting in the Ni-catalyzed C−H functionalization of **1a**; however, we have shown both these steps proceed at temperatures as low as 80 °C under stoichiometric conditions. In contrast, under catalytic conditions, much higher temperatures of 140−160 °C are required. We examined solutions during catalysis by ^{1}H NMR to try to observe the resting state

https://doi.org/10.1021/acs.organomet.1c00265
Organometallics XXXX, XXX, XXX−XXX

Scheme 12. Interconversion of Experimental Observed Intermediates in Ni(II)-Mediated C(sp^3)−H Arylation

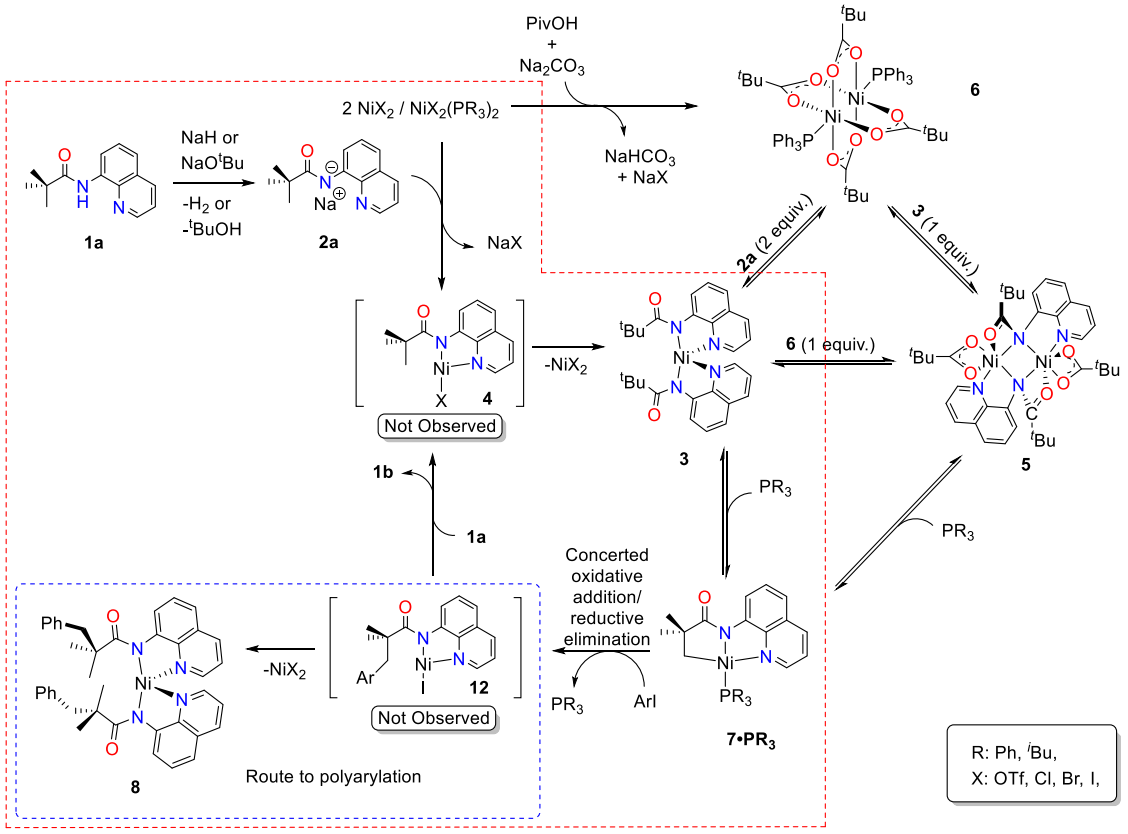

of the catalyst and better understand why such high temperatures were required for catalysis.

The initial attempt to observe a catalyst resting state used 20% $Ni(OTf)_2$ and PPh_3 to catalyze the reaction of **1a** with PhI and Na_2CO_3 as the base. Catalysis occurs at temperatures from 140 to 160 °C, but very careful attempts to observe a catalyst resting state by either ^1H, $^{31}P\{^1H\}$ and $^{19}F\{^1H\}$ NMR failed to detect relevant species. The ^1H NMR featured no peaks associated with Ni species, either diamagnetic or paramagnetic. Every peak in the ^1H spectrum could be assigned to either diamagnetic reagents and products that did not contain Ni. Similarly, the $^{31}P\{^1H\}$ NMR only showed PPh_3 and the ^{19}F NMR only showed free triflate anion at δ −78.2.

A similar experiment was done using **6·PPh$_3$** in lieu of $Ni(OTf)_2$ as the catalyst precursor. As the solution was heated up to 140−160 °C the ^1H NMR signal for **6·PPh$_3$** in dioxane disappeared, with no new resonances appearing to replace over the range of −250 to +250 ppm. To test if the catalyst resting state was insoluble, a portion of the reaction mixture was filtered through Celite. After continuing to heat at 140−160 °C the rate of catalysis of the filtered and unfiltered samples showed no difference, consistent with a soluble resting state of the catalyst. To confirm the unobservable resting state is caused by reaction with Na_2CO_3, a control experiment was carried out by heating **6·PPh$_3$** and DMSO in dioxane with and without added Na_2CO_3. The ^1H NMR of the solution of **6·PPh$_3$** heated with Na_2CO_3 shows no peaks associated with any Ni species. A hypothesis for the lack of observable resting state in these reaction was that the Ni(II) precursors were reacting with Na_2CO_3 to give dioxane soluble Ni carbonate species. Such a complex would be ^1H, ^{31}P, and ^{19}F NMR-silent. This result suggests not only that Na_2CO_3 fails to effectively deprotonate **1a** but also that the carbonate anion binds to Ni(II) to generate a lower energy species, thus increasing the temperature necessary for catalysis. Previously published DFT studies suggested that the carbonate bound to Ni(II) along with the 8-AQ^{piv} ligand was the resting state for catalysis. We found no experimental evidence for 8-AQ^{piv} binding in the resting state.

Alternatives for Na_2CO_3. With the hypothesis that Na_2CO_3 was deleterious to catalysis, NaO^{t}Bu was investigated as an alternative base. It is relatively cost-effective for synthetic applications, and with a pK_a of 17−18,[102] it is a stronger base than Na_2CO_3 which has a pK_a of ca. 10.5.[103] NaO^{t}Bu is suitable for the deprotonation of **1a**, which is anticipated to have a pK_a around 10. The reaction of NaO^{t}Bu with **1a** and $(Ph_3P)_2NiI_2$ in dioxane immediately generated the distinct paramagnetic ^1H NMR signals for **3** at room temperature. This is in contrast to the same reaction attempted with Na_2CO_3 in lieu of NaO^{t}Bu as the base, where no reaction is observed even with heating.

The use of NaO^{t}Bu as the base under catalytic conditions improved catalyst performance and allowed significantly higher catalyst turnover under milder conditions. The reaction requires an excess of NaO^{t}Bu. Using 1 equiv deprotonates the 8-AQ NH, and any ^{t}BuOH produced appears to sequester an additional equivalent of NaO^{t}Bu in the reaction. Catalysis was observed as low at 100 °C, rather than 140−160 °C as was required with Na_2CO_3. However, catalysis still proceeds cleanly at higher temperatures, and using 10 equiv of NaO^{t}Bu allowed a 94% conversion to trifunctionalized product **1d** after workup, as shown in Scheme 11. The reaction crude showed only 6% remaining difunctionalized product **1c** and no detectable **1b** or **1a** by NMR. This is a net functionalization

https://doi.org/10.1021/acs.organomet.1c00265
Organometallics XXXX, XXX, XXX−XXX

of 98% of the available Me groups in the sample. Neither carboxylic acids, such as pivalic acid, nor phosphine additives were necessary for catalysis under these conditions. The increase in reactivity compared to systems that utilize Na_2CO_3 is dramatic. The most closely related reactions using Na_2CO_3 noted in the literature involve more activated substrates and a net functionalization of only 69% of the available Me groups in the sample.[23]

CONCLUSION

Previous experimental studies related to the Ni-catalyzed arylation of C(sp^3)−H bonds in *N*-(quinolin-8-yl)pivalamide (**1a**) have largely focused on the mechanistic steps that were believed to be rate-determining, namely, the C−H activation and subsequent oxidative addition to Ni(II). Likewise, previous computational studies also suggested these steps and the rate-determining steps in catalysis. All the former proposed mechanisms are closely related to those suggested for heavier metals, thus the focus on diamagnetic mononuclear intermediates. These works left a few key questions remaining regarding the actual experimental mechanism. The calculated reaction barriers were smaller than would be expected for a reaction that requires heating to 140−160 °C, and no experimental resting state had ever been reported for these reactions. Our experimental results show that the intermediates prior to C−H activation and after functionalization are all paramagnetic Ni(II) species, such as **3**, **5**, **8**, and **9**. Both the C−H activation and oxidative addition steps, previously proposed as likely rate-determining steps, occur stoichiometrically at 80 °C, a temperature much lower than the temperatures required for catalysis. Under the original catalytic conditions employing Na_2CO_3 as a base, the deprotonation and binding of **1a** appears to be rate-limiting, due to the insufficient basicity of Na_2CO_3 and its propensity to react with catalytic precursors like **6** to yield less reactive, NMR-silent, off-cycle resting state. From these mechanistic insights, a simple approach to improved catalysis in these systems was developed using readily available NaO^{t}Bu as the base. A summary of the observed mechanistic manifolds is shown in Scheme 12. Catalysis is much more effective with NaO^{t}Bu, and additional additives such as PPh_3 or pivalic acid proved unnecessary and yield no improvement to catalysis. The intermediates outside the red box are only relevant to catalysis done in the presence of pivalic acid. Further studies are needed to probe the expanded scope of C−H activation reactions afforded by alternative bases like NaO^{t}Bu, as well as to determine possible alternative mechanisms derived from reaction of Ni species with this species acting in roles other than simply bases. These studies are currently underway. The use of Na_2CO_3 as a base is so ubiquitous in Ni catalyzed reactions that it raises the question if it is hindering catalysis in a vast number of unrelated systems.

ASSOCIATED CONTENT

Supporting Information

The Supporting Information is available free of charge at https://pubs.acs.org/doi/10.1021/acs.organomet.1c00265.

Detailed syntheses, characterization data and NMR spectra, kinetic data, computational details, and select crystallographic data (PDF)

Cartesian coordinates for the calculated structures (XYZ)

Accession Codes

CCDC 2055354, 2055446, 2055449, 2055452, 2055455, and 2055459 contain the supplementary crystallographic data for this paper. These data can be obtained free of charge via www.ccdc.cam.ac.uk/data_request/cif, or by emailing data_request@ccdc.cam.ac.uk, or by contacting The Cambridge Crystallographic Data Centre, 12 Union Road, Cambridge CB2 1EZ, UK; fax: +44 1223 336033.

AUTHOR INFORMATION

Corresponding Author

Samuel A. Johnson − *Department of Chemistry and Biochemistry, University of Windsor, Windsor, Ontario N9B 3P4, Canada;* orcid.org/0000-0001-6856-0416; Phone: +1 519 253 3000; Email: sjohnson@uwindsor.ca; Fax: +1 519 973 7098

Author

Junyang Liu − *Department of Chemistry and Biochemistry, University of Windsor, Windsor, Ontario N9B 3P4, Canada*

Complete contact information is available at: https://pubs.acs.org/10.1021/acs.organomet.1c00265

Notes

The authors declare no competing financial interest.

ACKNOWLEDGMENTS

S.A.J. acknowledges the Natural Sciences and Engineering Research Council (NSERC) of Canada for funding and SHARCNET and Compute Canada for computational resources.

REFERENCES

(1) Daugulis, O.; Roane, J.; Tran, L. D. Bidentate, Monoanionic Auxiliary-Directed Functionalization of Carbon−Hyrogen Bonds. *Acc. Chem. Res.* **2015**, *48*, 1053−1064.

(2) Yan, J.-X.; Li, H.; Liu, X.-W.; Shi, J.-L.; Wang, X.; Shi, Z.-J. Palladium-Catalyzed C(sp^3)-H Activation: A Facile Method for theSynthesis of 3,4-Dihydroquinolinone Derivatives. *Angew. Chem., Int. Ed.* **2014**, *53*, 4945−4949.

(3) Shang, R.; Ilies, L.; Matsumoto, A.; Nakamura, E. *β*-Arylation of Carboxamides via Iron-Catalyzed C(sp^3)−H Bond Activation. *J. Am. Chem. Soc.* **2013**, *135*, 6030−6032.

(4) Daugulis, O.; Do, H.-Q.; Shabashov, D. Palladium- and Copper-Catalyzed Arylation of Carbon−Hydrogen Bonds. *Acc. Chem. Res.* **2009**, *42*, 1074−1086.

(5) Waltz, K. M.; Hartwig, J. F. Selective Functionalization of Alkanes by Transition-Metal Boryl Complexes. *Science* **1997**, *277*, 211−213.

(6) Arndtsen, B. A.; Bergman, R. G.; Mobley, T. A.; Peterson, H. H. Selective Intermolecular Carbon−Hydrogen Bond Activation by Synthetic Metal Complexes in Homogeneous Solution. *Acc. Chem. Res.* **1995**, *28*, 154−162.

(7) Harry, N. A.; Saranya, S.; Ujwaldev, S. M.; Anilkumar, G. Recent advances and prospects in nickel catalyzed C−H activation. *Catal. Sci. Technol.* **2019**, *9*, 1726−1743.

(8) Gandeepan, P.; Muller, T.; Zell, D.; Cera, G.; Warratz, S.; Ackermann, L. 3d Transition Metals for C-H Activation. *Chem. Rev.* **2019**, *119*, 2192−2452.

(9) Mishra, A. A.; Subhedar, D.; Bhanage, B. M. Nickel, Cobalt and Palladium Catalysed C-H Functionalization of Un-Activated C(sp^3)-H Bond. *Chem. Rec.* **2019**, *19*, 1829−1857.

(10) St John-Campbell, S.; Bull, J. A. Base Metal Catalysis in Directed C(sp^3)-H Functionalisation. *Adv. Synth. Catal.* **2019**, *361*, 3662−3682.

(11) Khake, S. M.; Chatani, N. Chelation-Assisted Nickel-Catalyzed C-H Functionalizations. *Trends Chem.* **2019**, *1*, 524−539.
(12) Liu, Y. H.; Xia, Y. N.; Shi, B. F. Ni-Catalyzed Chelation-Assisted Direct Functionalization of Inert C-H Bonds. *Chin. J. Chem.* **2020**, *38*, 635−662.
(13) Rej, S.; Das, A.; Chatani, N. Strategic evolution in transition metal-catalyzed directed C−H bond activation and future directions. *Coord. Chem. Rev.* **2021**, *431*, 213683.
(14) Chirik, P.; Morris, R. Getting Down to Earth: The Renaissance of Catalysis with Abundant Metals. *Acc. Chem. Res.* **2015**, *48*, 2495−2495.
(15) Smith, M. B.; March, J. *Advanced Organic Chemistry*, 6th ed.; Wiley, 2007.
(16) Tobisu, M.; Chatani, N. Remote Control by Steric Effects. *Science* **2014**, *343*, 850−851.
(17) Shaw, M. H.; Shurtleff, V. W.; Terrett, J. A.; Cuthbertson, J. D.; MacMillan, D. W. C. Native functionality in triple catalytic cross-coupling: sp3 C−H bonds as latent nucleophiles. *Science* **2016**, *352*, 1304−1308.
(18) Kleiman, J. P.; Dubeck, M. The Preparation of Cyclopentadienyl [o-(Phenylazo)Phenyl]Nickel. *J. Am. Chem. Soc.* **1963**, *85*, 1544−1545.
(19) Murai, S.; Kakiuchi, F.; Sekine, S.; Tanaka, T.; Kamatani, A.; Sonoda, M.; Chatani, N. Efficient catalytic addition of aromatic carbon-hyrogen bonds to olefins. *Nature* **1993**, *366*, 529−531.
(20) Daugulis, O.; Roane, J.; Tran, L. D. Bidentate, Monoanionic Auxiliary-Directed Functionalization of Carbon− Hydrogen Bonds. *Acc. Chem. Res.* **2015**, *48*, 1053−1064.
(21) Shiota, H.; Ano, Y.; Aihara, Y.; Fukumoto, Y.; Chatani, N. Nickel-Catalyzed Chelation-Assisted Transformations Involving Ortho C-H Bond Activation: Regioselective Oxidative Cycloaddition of Aromatic Amides to Alkynes. *J. Am. Chem. Soc.* **2011**, *133*, 14952−14955.
(22) Castro, L. C. M.; Chatani, N. Nickel Catalysts/N,N'-Bidentate Directing Groups: An Excellent Partnership inDirected CH Activation Reactions. *Chem. Lett.* **2015**, *44*, 410−421.
(23) Aihara, Y.; Chatani, N. Nickel-Catalyzed Direct Arylation of $C(sp^3)$-H Bonds in Aliphatic Amides via Bidentate-Chelation Assistance. *J. Am. Chem. Soc.* **2014**, *136*, 898−901.
(24) Li, M.; Dong, J.; Huang, X.; Li, K.; Wu, Q.; Song, F.; You, J. Nickel-catalyzed chelation-assisted direct arylation of unactivated $C(sp^3)$−H bonds with aryl halides. *Chem. Commun.* **2014**, *50*, 3944.
(25) Aihara, Y.; Tobisu, M.; Fukumoto, Y.; Chatani, N. Ni(II)-Catalyzed Oxidative Coupling between $C(sp^2)$−H in Benzamides and $C(sp^3)$−H in Toluene Derivatives. *J. Am. Chem. Soc.* **2014**, *136*, 15509−15512.
(26) Aihara, Y.; Wuelbern, J.; Chatani, N. The Nickel(II)-Catalyzed Direct Benzylation, Allylation, Alkylation, and Methylation of CH Bonds in AromaticAmides Containing an 8-Aminoquinoline Moiety as the Directing Group. *Bull. Chem. Soc. Jpn.* **2015**, *88*, 438−446.
(27) Wu, X.; Zhao, Y.; Ge, H. Nickel-Catalyzed Site-Selective Alkylation of Unactivated $C(sp^3)$-H Bonds. *J. Am. Chem. Soc.* **2014**, *136*, 1789−1792.
(28) Wu, X.; Zhao, Y.; Ge, H. Direct Aerobic Carbonylation of $C(sp^2)$−H and $C(sp^3)$-H Bonds through Ni/Cu Synergistic Catalysis with DMF as the Carbonyl Source. *J. Am. Chem. Soc.* **2015**, *137*, 4924−4927.
(29) Liu, Y.-J.; Zhang, Z.-Z.; Yan, S.-Y.; Liu, Y.-H.; Shi, B.-F. Ni(II)/BINOL-catalyzed alkenylation of unactivated $C(sp^3)$−H bonds. *Chem. Commun.* **2015**, *51*, 7899.
(30) Maity, S.; Agasti, S.; Earsad, A. M.; Hazra, A.; Maiti, D. Nickel-Catalyzed Insertion of Alkynes and Electron-Deficient Olefins into Unactivated sp3 C-H Bonds. *Chem. - Eur. J.* **2015**, *21*, 11320−11324.
(31) Li, M.; Yang, Y.; Zhou, D.; Wan, D.; You, J. Nickel-Catalyzed Addition-Type Alkenylation of Unactivated, Aliphatic C−H Bonds with Alkynes: A Concise Route to Polysubstituted γ-Butyrolactones. *Org. Lett.* **2015**, *17*, 2546−2549.
(32) Misal Castro, L. C.; Obata, A.; Aihara, Y.; Chatani, N. Chelation-Assisted Nickel-Catalyzed OxidativeAnnulation via Double C-H Activation/Alkyne Insertion Reaction. *Chem. - Eur. J.* **2016**, *22*, 1362−1367.
(33) Cheng, Y.; Wu, Y.; Tan, G.; You, J. Nickel Catalysis Enables Oxidative $C(sp^2)$−H/$C(sp^2)$−H Cross-Coupling Reactions between Two Heteroarenes. *Angew. Chem., Int. Ed.* **2016**, *55*, 12275−12279.
(34) He, Z.; Huang, Y. Diverting C-H Annulation Pathways: Nickel-Catalyzed Dehydrogenative Homologation of Aromatic Amides. *ACS Catal.* **2016**, *6*, 7814−7823.
(35) Uemura, T.; Yamaguchi, M.; Chatani, N. Phenyltrimethylammonium Salts as Methylation Reagents in the Nickel-Catalyzed Methylation of C-H Bonds. *Angew. Chem., Int. Ed.* **2016**, *55*, 3162−3165.
(36) Honeycutt, A. P.; Hoover, J. M. Nickel-Catalyzed Oxidative Decarboxylative (Hetero)Arylation of Unactivated C−H Bonds: Ni and Ag Synergy. *ACS Catal.* **2017**, *7*, 4597−4601.
(37) Luo, F.-X.; Cao, Z.-C.; Zhao, H.-W.; Wang, D.; Zhang, Y.-F.; Xu, X.; Shi, Z.-J. Nickel-Catalyzed Oxidative Coupling of Unactivated C(sp3)-H Bonds in Aliphatic Amides with Terminal Alkynes. *Organometallics* **2017**, *36*, 18−21.
(38) Wang, X.; Xie, P.; Qiu, R.; Zhu, L.; Liu, T.; Li, Y.; Iwasaki, T.; Au, C.-T.; Xu, X.; Xia, Y.; Yin, S.-F.; Kambe, N. Nickel-catalysed direct alkylation of thiophenes via double $C(sp^3)$−H/$C(sp^2)$−H bond cleavage: the importance of KH^3PO_4. *Chem. Commun.* **2017**, *53*, 8316.
(39) Tan, G.; Zhang, L.; Liao, X.; Shi, Y.; Wu, Y.; Yang, Y.; You, J. Copper- or Nickel-Enabled Oxidative Cross-Coupling of Unreactive $C(sp^3)$-H Bonds with Azole $C(sp^2)$-H Bonds: Rapid Access to β-Azolyl Propanoic Acid Derivatives. *Org. Lett.* **2017**, *19*, 4830−4833.
(40) Lin, C.; Chen, Z.; Liu, Z.; Zhang, Y. Nickel-Catalyzed Stereoselective Alkenylation of $C(sp^3)$-H Bonds with Terminal Alkynes. *Org. Lett.* **2017**, *19*, 850−853.
(41) Liu, X.; Mao, G.; Qiao, J.; Xu, C.; Liu, H.; Ma, J.; Sun, Z.; Chu, W. Nickel-catalyzed C−H bond trifluoromethylation of 8-amino-quinoline derivatives by acyl-directed functionalization. *Org. Chem. Front.* **2019**, *6*, 1189.
(42) Skhiri, A.; Chatani, N. Nickel-Catalyzed Reaction of Benzamides with Bicylic Alkenes: Cleavage of C-H and C-N Bonds. *Org. Lett.* **2019**, *21*, 1774−1778.
(43) Derosa, J.; van der Puyl, V. A.; Tran, V. T.; Liu, M.; Engle, K. M. Directed nickel-catalyzed 1,2-dialkylation of alkenyl carbonyl compounds. *Chem. Sci.* **2018**, *9*, 5278.
(44) Wang, X.; Qiu, R.; Yan, C.; Reddy, V. P.; Zhu, L.; Xu, X.; Yin, S.-F. Nickel-Catalyzed Direct Thiolation of $C(sp^3)$−H Bonds in Aliphatic Amides. *Org. Lett.* **2015**, *17*, 1970−1973.
(45) Obata, A.; Ano, Y.; Chatani, N. Nickel-catalyzed C−H/N−H annulation of aromatic amides with alkynes in the absence of a specific chelation system. *Chem. Sci.* **2017**, *8*, 6650.
(46) Wu, X.; Zhao, Y.; Ge, H. Nickel-Catalyzed Site-Selective Amidation of Unactivated $C(sp^3)$-H Bonds. *Chem. - Eur. J.* **2014**, *20*, 9530−9533.
(47) Ye, X.; Petersen, J. L.; Shi, X. Nickel-catalyzed directed sulfenylation of sp^2 and sp^3 C−H bonds. *Chem. Commun.* **2015**, *51*, 7863−7866.
(48) Lin, C.; Yu, W.; Yao, J.; Wang, B.; Liu, Z.; Zhang, Y. Nickel-Catalyzed Direct Thioetherification of β-$C(sp^3)$−H Bonds of Aliphatic Amides. *Org. Lett.* **2015**, *17*, 1340−1343.
(49) Yan, S.-Y.; Liu, Y.-J.; Liu, B.; Liu, Y.-H.; Zhang, Z.-Z.; Shi, B.-F. Nickel-catalyzed direct thiolation of unactivated $C(sp^3)$−H bonds with disulfides. *Chem. Commun.* **2015**, *51*, 7341−7344.
(50) Yokota, A.; Chatani, N. Ni(II)-Catalyzed Sulfonylation of ortho CH Bonds in AromaticAmides Utilizing an N,N-Bidentate Directing Group. *Chem. Lett.* **2015**, *44*, 902−904.
(51) Aihara, Y.; Chatani, N. Nickel-Catalyzed Reaction of C−H Bonds in Amides with I2: ortho- Iodination via the Cleavage of $C(sp^2)$-H Bonds and Oxidative Cyclization to β-Lactams via the Cleavage of $C(sp^3)$−H Bonds. *ACS Catal.* **2016**, *6*, 4323−4329.
(52) Iwasaki, M.; Miki, N.; Tsuchiya, Y.; Nakajima, K.; Nishihara, Y. Synthesis of Benzoisoselenazolone Derivatives by Nickel-Catalyzed

https://doi.org/10.1021/acs.organomet.1c00265
Organometallics XXXX, XXX, XXX−XXX

Dehydrogenative Direct Selenation of C(sp^2)-H Bonds with Elemental Selenium in Air. *Org. Lett.* **2017**, *19*, 1092−1095.
(53) van der Puyl, V. A.; Derosa, J.; Engle, K. M. Directed, Nickel-Catalyzed Umpolung 1,2-Carboamination of Alkenyl Carbonyl Compounds. *ACS Catal.* **2019**, *9*, 224−229.
(54) Xu, S.; Takamatsu, K.; Hirano, K.; Miura, M. Synthesis of Seven-Membered Benzolactones by Nickel-Catalyzed C-H Coupling of Benzamides with Oxetanes. *Chem. - Eur. J.* **2019**, *25*, 9400−9404.
(55) Yu, L.; Chen, X.; Liu, D.; Hu, L.; Yu, Y.; Huang, H.; Tan, Z.; Gui, Q. Direct Synthesis of Primary Anilines via Nickel-mediated C(sp2)- H Aminations. *Adv. Synth. Catal.* **2018**, *360*, 1346−1351.
(56) Shi, Y.; Li, M.-S.; Zhang, F.; Chen, B. Nickel(II)-catalyzed tandem C(sp2)−H bond activation and annulation of arenes with gem-dibromoalkenes. *RSC Adv.* **2018**, *8*, 28668.
(57) Gorelsky, S. I.; Lapointe, D.; Fagnou, K. Analysis of the Palladium-Catalyzed (Aromatic)C-H Bond Metalation−Deprotonation Mechanism Spanning the Entire Spectrum of Arenes. *J. Org. Chem.* **2012**, *77*, 658−668.
(58) Davies, D. L.; Donald, S. M. A.; Macgregor, S. A. Computational Study of the Mechanism of Cyclometalation by Palladium Acetate. *J. Am. Chem. Soc.* **2005**, *127*, 13754−13755.
(59) Liu, J.-B.; Tian, Y.-Y.; Zhang, X.; Wang, L.-L.; Chen, D.-Z. A computational mechanistic study of Pd(II)- catalyzed γ-C(sp^3)−H olefination/cyclization of amines: the roles of bicarbonate and ligand effect. *Dalton Trans.* **2018**, *47*, 4893−4901.
(60) Singh, S.; K, S.; Sunoj, R. B. Aliphatic C(sp^3)-H Bond Activation Using Nickel Catalysis: Mechanistic Insights on Regioselective Arylation. *J. Org. Chem.* **2017**, *82*, 9619−9626.
(61) Omer, H. M.; Liu, P. Computational Study of Ni-Catalyzed C-H Functionalization: Factors That Control the Competition of Oxidative Addition and Radical Pathways. *J. Am. Chem. Soc.* **2017**, *139*, 9909−9920.
(62) Beattie, D. D.; Grunwald, A. C.; Perse, T.; Schafer, L. L.; Love, J. A. Understanding Ni(II)-Mediated C(sp^3)−H Activation: Tertiary Ureas as Model Substrates. *J. Am. Chem. Soc.* **2018**, *140*, 12602−12610.
(63) Hill, E. A.; Zhao, N.; Filatov, A. S.; Anderson, J. S. Nickel(II)-methyl complexes adopting unusual seesaw geometries. *Chem. Commun.* **2020**, *56*, 7861−7864.
(64) Graziani, R.; Vidali, M.; Casellato, U.; Vigato, P. A. Preparation and crystal structure of a nickel (II)-Uranyl(VI) binuclear chelate. *Transition Met. Chem.* **1978**, *3*, 99−103.
(65) Li, J.; Tian, D.; Song, H.; Wang, C.; Zhu, X.; Cui, C.; Cheng, J. Synthesis, Structures, and Reactivity of Nickel Complexes Incorporating Sulfonamido-Imine Ligands. *Organometallics* **2008**, *27*, 1605−1611.
(66) Ghannam, J.; Al Assil, T.; Pankratz, T. C.; Lord, R. L.; Zeller, M.; Lee, W. T. A Series of 4- and 5-Coordinate Ni(II) Complexes: Synthesis, Characterization, Spectroscopic, and DFT Studies. *Inorg. Chem.* **2018**, *57*, 8307−8316.
(67) Zhang, S. K.; Struwe, J.; Hu, L.; Ackermann, L. Nickela-electrocatalyzed C−H Alkoxylation with Secondary Alcohols: Oxidation-Induced Reductive Elimination at Nickel(III). *Angew. Chem., Int. Ed.* **2020**, *59*, 3178−3183.
(68) He, Z.; Huang, Y. Diverting C−H Annulation Pathways: Nickel-Catalyzed Dehydrogenative Homologation of Aromatic Amides. *ACS Catal.* **2016**, *6*, 7814−7823.
(69) Maity, S.; Kancherla, R.; Dhawa, U.; Hoque, E.; Pimparkar, S.; Maiti, D. Switch to Allylic Selectivity in Cobalt-Catalyzed Dehydrogenative Heck Reactions with Unbiased Aliphatic Olefins. *ACS Catal.* **2016**, *6*, 5493−5499.
(70) Chatturgoon, T.; Akerman, M. P. X-ray and DFT-calculated structures of bis[N-(quinolin-8-yl)benzamidato-κ^2-N,N']copper(II). *Acta Crystallogr., Sect. C: Struct. Chem.* **2016**, *72*, 234.
(71) Shilov, A. E.; Shul'pin, G. B. Activation of C-H Bonds by Metal Complexes. *Chem. Rev.* **1997**, *97*, 2879−2932.
(72) Macaulay, C. M.; Samolia, M.; Ferguson, M. J.; Sydora, O. L.; Ess, D. H.; Stradiotto, M.; Turculet, L. Synthetic investigations of low-coordinate (N-phosphino-amidinate) nickel chemistry: agostic alkyl complexes and benzene insertion into Ni−H. *Dalton Trans.* **2020**, *49*, 4811−4816.
(73) Calvert, R. B.; Shapley, J. R. Decacarbonyl(methyl)-hydrotriosmium: NMR Evidence for a carbon··hydrogen··osmium Interaction. *J. Am. Chem. Soc.* **1978**, *100*, 7726−7727.
(74) Green, M. L. H.; Hughes, A. K.; Popham, N. A.; Stephens, A. H. H.; Wong, L.-L. Nuclear magnetic resonance studies on partially deuteriated transition metal−methyl derivatives. *J. Chem. Soc., Dalton Trans.* **1992**, 3077−3082.
(75) Kitiachvili, K. D.; Mindiola, D. J.; Hillhouse, G. L. Preparation of stable alkyl complexes of Ni(I) and their one-electron oxidation to Ni(II) complex cations. *J. Am. Chem. Soc.* **2004**, *126*, 10554−10555.
(76) Kogut, E.; Zeller, A.; Warren, T. H.; Strassner, T. Structure and dynamics of neutral beta-h agostic nickel alkyls: A combined experimental and theoretical study. *J. Am. Chem. Soc.* **2004**, *126*, 11984−11994.
(77) Scherer, W.; Herz, V.; Bruck, A.; Hauf, C.; Reiner, F.; Altmannshofer, S.; Leusser, D.; Stalke, D. The Nature of beta-Agostic Bonding in Late-Transition-Metal Alkyl Complexes. *Angew. Chem., Int. Ed.* **2011**, *50*, 2845−2849.
(78) Xu, H. W.; White, P. B.; Hu, C. H.; Diao, T. N. Structure and Isotope Effects of the beta-H Agostic (alpha-Diimine)Nickel Cation as a Polymerization Intermediate. *Angew. Chem., Int. Ed.* **2017**, *56*, 1535−1538.
(79) Mitoraj, M. P.; Babashkina, M. G.; Robeyns, K.; Sagan, F.; Szczepanik, D. W.; Seredina, Y. V.; Garcia, Y.; Safin, D. A. Chameleon-like Nature of Anagostic Interactions and Its Impact on Metalloaromaticity in Square-Planar Nickel Complexes. *Organometallics* **2019**, *38*, 1973−1981.
(80) Huynh, H. V.; Wong, L. R.; Ng, P. S. Anagostic interactions and catalytic activities of sterically bulky benzannulated N-heterocyclic carbene complexes of nickel(II). *Organometallics* **2008**, *27*, 2231−2237.
(81) Roy, P.; Bour, J. R.; Kampf, J. W.; Sanford, M. S. Catalytically Relevant Intermediates in the Ni-Catalyzed C(sp^2)−H and C(sp^3)−H Functionalization of Aminoquinoline Substrates. *J. Am. Chem. Soc.* **2019**, *141*, 17382−17387.
(82) Ghorai, D.; Finger, L. H.; Zanoni, G.; Ackermann, L. Bimetallic Nickel Complexes for Aniline C-H Alkylations. *ACS Catal.* **2018**, *8*, 11657−11662.
(83) Somerville, R. J.; Hale, L. V. A.; Gómez-Bengoa, E.; Burés, J.; Martin, R. Intermediacy of Ni-Ni Species in sp^2 C-O Bond Cleavage of Aryl Esters: Relevance in Catalytic C-Si Bond Formation. *J. Am. Chem. Soc.* **2018**, *140*, 8771−8780.
(84) Jiang, Y.; Zhang, S.-Q.; Cao, F.; Zou, J.-X.; Yu, J.-L.; Shi, B.-F.; Hong, X.; Wang, Z. Unexpected Stability of CO-Coordinated Palladacycle in Bidentate Auxiliary Directed C(sp^3)−H Bond Activation: A Combined Experimental and Computational Study. *Organometallics* **2019**, *38*, 2022−2030.
(85) Zhang, S.-Y.; Li, Q.; He, G.; Nack, W. A.; Chen, G. Pd-Catalyzed Monoselective ortho-C−H Alkylation of N-Quinolyl Benzamides: Evidence for Stereoretentive Coupling of Secondary Alkyl Iodides. *J. Am. Chem. Soc.* **2015**, *137*, 531−539.
(86) Czyz, M. L.; Weragoda, G. K.; Horngren, T. H.; Connell, T. U.; Gomez, D.; O'Hair, R. A. J.; Polyzos, A. Photoexcited Pd(II) auxiliaries enable light-induced control in C(sp^3)−H bond functionalisation. *Chem. Sci.* **2020**, *11*, 2455.
(87) Shabashov, D.; Daugulis, O. Auxiliary-Assisted Palladium-Catalyzed Arylation and Alkylation of sp^2 and sp^3 Carbon-Hydrogen Bonds. *J. Am. Chem. Soc.* **2010**, *132*, 3965−3972.
(88) Meng, Y.-Y.; Si, X.-J.; Song, Y.-Y.; Zhou, H.-M.; Xu, F. Palladium-catalyzed decarbonylative annulation of phthalimides with arynes: direct construction of phenanthridinones. *Chem. Commun.* **2019**, *55*, 9507−9510.
(89) Deb, A.; Singh, S.; Seth, K.; Pimparkar, S.; Bhaskararao, B.; Guin, S.; Sunoj, R. B.; Maiti, D. Experimental and Computational Studies on Remote γ-C(sp^3)−HSilylation and Germanylation of Aliphatic Carboxamides. *ACS Catal.* **2017**, *7*, 8171−8175.

https://doi.org/10.1021/acs.organomet.1c00265
Organometallics XXXX, XXX, XXX−XXX

(90) Zhang, T.; Liu, S.; Zhu, L.; Liu, F.; Zhong, K.; Zhang, Y.; Bai, R.; Lan, Y. Theoretical study of FMO adjusted C-H cleavage and oxidative addition in nickel catalysed C-H arylation. *Commun. Chem.* **2019**, *2*, 31.
(91) Ackermann, L. Carboxylate-Assisted Transition-Metal-Catalyzed C-H Bond Functionalizations: Mechanism and Scope. *Chem. Rev.* **2011**, *111*, 1315−1345.
(92) Rousseaux, S.; Gorelsky, S. I.; Chung, B. K. W.; Fagnou, K. Investigation of the Mechanism of C(sp^3)-H Bond Cleavage in Pd(0)-Catalyzed Intramolecular Alkane Arylation Adjacent to Amides and Sulfonamides. *J. Am. Chem. Soc.* **2010**, *132*, 10692−10705.
(93) Balcells, D.; Clot, E.; Eisenstein, O. C−H Bond Activation in Transition Metal Species from a Computational Perspective. *Chem. Rev.* **2010**, *110*, 749−823.
(94) Boutadla, Y.; Davies, D. L.; Macgregor, S. A.; Poblador-Bahamonde, A. I. Mechanisms of C−H bond activation: rich synergy between computation and experiment. *Dalton Trans.* **2009**, 5820−5831. and references therein.
(95) Gutsulyak, D. M.; Piers, W. E.; Borau-Garcia, J.; Parvez, M. Activation of Water, Ammonia, and Other Small Molecules by $PC_{carbene}P$ Nickel Pincer Complexes. *J. Am. Chem. Soc.* **2013**, *135*, 11776−11779.
(96) LaPierre, E. A.; Piers, W. E.; Spasyuk, D. M.; Bi, D. W. Activation of Si−H bonds across the nickel carbene bond in electron rich nickel $PC_{carbene}P$ pincer complexes. *Chem. Commun.* **2016**, *52*, 1361.
(97) Schultz, M.; Eisenträger, F.; Regius, C.; Rominger, F.; Hanno-Igels, P.; Jakob, P.; Gruber, I.; Hofmann, P. Crowded Diphosphinomethane Ligands in Catalysis: $[(R_2PCH_2PR_2\text{-}\kappa^2P)\text{-}NiR']^+$ Cations for Ethylene Polymerization without Activators. *Organometallics* **2012**, *31*, 207−224.
(98) Tsou, T. T.; Kochi, J. K. Mechanism of Oxidative Addition. Reaction of Nickel(O) Complexes with Aromatic Halides. *J. Am. Chem. Soc.* **1979**, *101*, 6319−6332.
(99) Amatore, C.; Pfluger, F. Mechanism of oxidative addition of palladium(0) with aromatic iodides in toluene, monitored at ultramicroelectrodes. *Organometallics* **1990**, *9*, 2276−2282.
(100) Khake, S. M.; Jagtap, R. A.; Dangat, Y. B.; Gonnade, R. G.; Vanka, K.; Punji, B. Mechanistic Insights into Pincer-Ligated Palladium-Catalyzed Arylation of Azoles with Aryl Iodides: Evidence of a Pd^{II}−Pd^{IV}−Pd^{II} Pathway. *Organometallics* **2016**, *35*, 875−886.
(101) Pandiri, H.; Soni, V.; Gonnade, R. G.; Punji, B. Development of (quinolinyl)amido-based pincer palladium complexes: a robust and phosphinefree catalyst system for C−H arylation of benzothiazoles. *New J. Chem.* **2017**, *41*, 3543−3554.
(102) Dewick, P. M. Acids and Bases. In *Essentials of Organic Chemistry: For Students of Pharmacy, Medicinal Chemistry and Biological Chemistry*; John Wwiley & Sons. Ltd., 2006; pp 122−166.
(103) Windholz, M. In *The Merck Index an Encyclopedia of Chemicals, Drugs, And Biologicals*, 10th ed.; Merck, 1983.

https://doi.org/10.1021/acs.organomet.1c00265
Organometallics XXXX, XXX, XXX−XXX